Controlled Growth of Single-Walled Carbon Nanotubes from an Ordered Mesoporous Silica Template

ARTICLE *in* NANO LETTERS · MARCH 2003

Impact Factor: 13.59 · DOI: 10.1021/nl025880p

NANO LETTERS

2003
Vol. 3, No. 3
299−303

Controlled Growth of Single-Walled Carbon Nanotubes from an Ordered Mesoporous Silica Template

Limin Huang,[†] Shalom J. Wind,[‡] and Stephen P. O'Brien*,[†]

Department of Applied Physics & Applied Mathematics, Columbia University, New York, New York 10027, and IBM T. J. Watson Research Center, P.O. Box 218, Yorktown Heights, New York 10598

Received November 6, 2002; Revised Manuscript Received January 2, 2003

ABSTRACT

We have grown carbon nanotubes (CNTs) with controlled orientation and diameter (1–4 nm) from thermally stable, highly ordered mesoporous SiO_2 thin films by methane chemical vapor deposition (CVD). Controlled incorporation of an Fe precursor into one-dimensional (1D) and three-dimensional (3D) pore channels of mesoporous SiO_2 results in a nanostructure catalytically active for CNT growth and stable to typical CVD temperatures. Growth of CNTs starts within the mesoporous SiO_2, whose pore direction and pore dimension play an important role in controlling the orientation and diameter of the CNTs at the early stage of the growth. Lateral growth across micropatterned trenches results in oriented CNT assemblies with controlled tube dimension. The flexibility of constructing parallel nanotube assemblies and nanotube junctions by this simple method suggests its high potential for fabricating future integrated molecular electronic nanodevices.

Single-walled carbon nanotubes (SWNTs) are molecular wires that are of fundamental research interest and have shown promising electronic properties (depending on diameters and chirality) for future generations of integrated molecular electronic devices.[1−4] Such integration requires the ability to assemble individual SWNTs into desired architectures with controlled diameter and orientation. Of the methods of nanotube synthesis reported to date, only chemical vapor deposition CVD offers any sort of in-situ controls over position and orientation.[5−13] Some orientational control has been achieved through the use of external electric fields.[12,13] The orientation of nanotubes could arise from template-assisted assembly[5−9] or self-assembly with van der Waals interactions between nanotube themselves, nanotube and surroundings (e.g., silicon pillars),[10,11] and from the external electric fields.[12,13]

Defect-free SWNTs can be prepared by methane CVD at high temperatures (700−1000 °C) over catalyst nanoparticles (Fe, Mo) formed on high surface area supports (e.g., Al_2O_3 or SiO_2).[11,14,15] A "base growth" model with catalyst nanoparticles anchored in the supports during the growth process and a correlation on size matching between catalyst nanoparticles and nanotubes have also been established.[15−17] We postulated that if a thermally stable template is used that has a uniform pore size comparable to the diameters of SWNTs and an ordered pore structure within which catalyst nanoparticles are located, the methane CVD process may result in SWNTs with controlled diameter and orientation. An anodic alumina template with closely packed nanochannels has been successfully used to grow highly ordered arrays of MWNTs−the channel size (usually tens of nanometers) is too big to control the dimension of SWNTs, and only arrays with vertical orientation have been demonstrated.[8]

In this report, we used highly stable, mesoporous silica thin films with uniform and adjustable mesopore sizes of 2−6 nm (matching the SWNT size range) and preferentially oriented pore direction (with the (100) face running parallel to the substrate) as a template.[18,19] Catalyst precursors (e.g., Fe) are incorporated into the mesostructure during a sol−gel process, and, after calcination, nanometer-sized Fe oxide particles are produced within the mesoporous channels with the particle size limited by the channel dimension, which, in turn, control the size of carbon nanotubes grown by CVD. In addition, the direction of mesopores in the thin film also influences the orientation of carbon nanotubes grown beyond the channels. For this templating role to be effective, the stability of the mesophases at high temperature (>800 °C) during the CVD process is a key issue. Mesoporous alumina derived from $AlCl_3$/block copolymer system has been widely used as a support for catalysts; however, it has lower thermal stability compared with silica-based counterparts and it loses its intrinsic mesostructure, with only nonuniform macroporous structure being observed after high-temperature exposure,

* Corresponding author: so188@columbia.edu
[†] Columbia University.
[‡] IBM T. J. Watson Research Center.

10.1021/nl025880p CCC: $25.00
Published on Web 02/05/2003

leaving the resultant CNT orientation uncontrollable.[16] High catalyst doping in mesoporous silica can cause framework instability due to possible severe leaching of catalyst species from the mesostructure at high temperature. However, highly doped mesoporous silica films have been reported to successfully grow aligned MWNT arrays.[5] Therefore, the orientation probably results from the high density of the nanotubes and the resultant strong van der Waals interactions between them, instead of the templating role of the mesophase itself. In contrast, by controlling the Fe doping level and using a slow calcination process, the intrinsic mesostructure may be preserved at the condition where CVD is carried out. Furthermore, high-porosity mesoporous silica is compatible with current semiconductor industry, and it could be used as low-k dielectric materials.[19] Thus far, the controlled growth of SWNTs has yet to be reported from the intrinsic channels of stable mesoporous silica thin films.

We have developed a simple procedure that allows the lateral growth of oriented CNTs with controlled diameter from patterned mesoporous SiO_2 thin films, which are created by soft lithography.[6,20] The Fe doping level was controlled to ensure the mesoporous silica stability up to 850 °C without the loss of their mesostructures. Mesoporous silica with different pore sizes has been used to study the effect of pore size on the dimensions of the nanotubes. This simple method offers a high flexibility in constructing complex nanotube assemblies.

Fe-doped mesoporous SiO_2 precursor solutions were prepared by mixing tetraethoxysilane (TEOS), surfactant (Pluronic P123, $EO_{20}PO_{70}EO_{20}$, or Pluronic F127, $EO_{106}PO_{70}EO_{106}$, or Brij56, $C_{16}H_{33}(OCH_2CH_2)_{10}OH$), 0.1 M HCl, water, ethanol, and certain amount of inorganic Fe salt ($FeCl_3 \cdot 6H_2O$) with molar ratio of 1: 0.003−0.008: 0.004−0.02: 5−10: 20−50: 0.008−0.05, according to a procedure reported elsewhere.[6,19] The as-prepared materials are labeled as Fe/SBA-15, Fe/SBA-16, and Fe/SBA-11 according to surfactant P123, F127, and Brij56, respectively (SBA-15 with 1D cylindrical pore channel, SBA-16 with 3D cubic structure, and SBA-11 with 3D cubic structure and smaller pore size). A controlled amount of Fe species (Fe/Si molar ratio of 0.8−5%) was incorporated to the mesoporous SiO_2 to ensure its thermal stability at high temperatures. Micropatterned thin films (thickness of 100−500 nm) with line spacing of 3 μm were prepared on silicon wafers by soft lithography using a PDMS mold with line micropatterns (Figure 1).[20] The samples were heated to 800 °C at a slow ramp rate (1 °C /min). CVD was carried out at 800−850 °C for 20 min to 1 h with the wafer placed in a 1-in.-diameter quartz tube furnace. Pure methane (500 cm^3/min) and hydrogen (50 cm^3/min) diluted in argon (500 cm^3/min) were used as reaction gases. Before the CVD, the samples were reduced in a H_2 (150 cm^3/min)/Ar (1000 cm^3/min) atmosphere at the same temperature for 0.5 h. The nanotube samples were characterized with atomic force microscopy (AFM, Nanoscope IIIa, Digital Instruments) and scanning electron microscopy (SEM, JEOL JSM-5600LV, or LEO 1500). The integrity of the mesoporous SiO_2 was characterized with X-ray diffraction (XRD, Scintag $\times 2$).

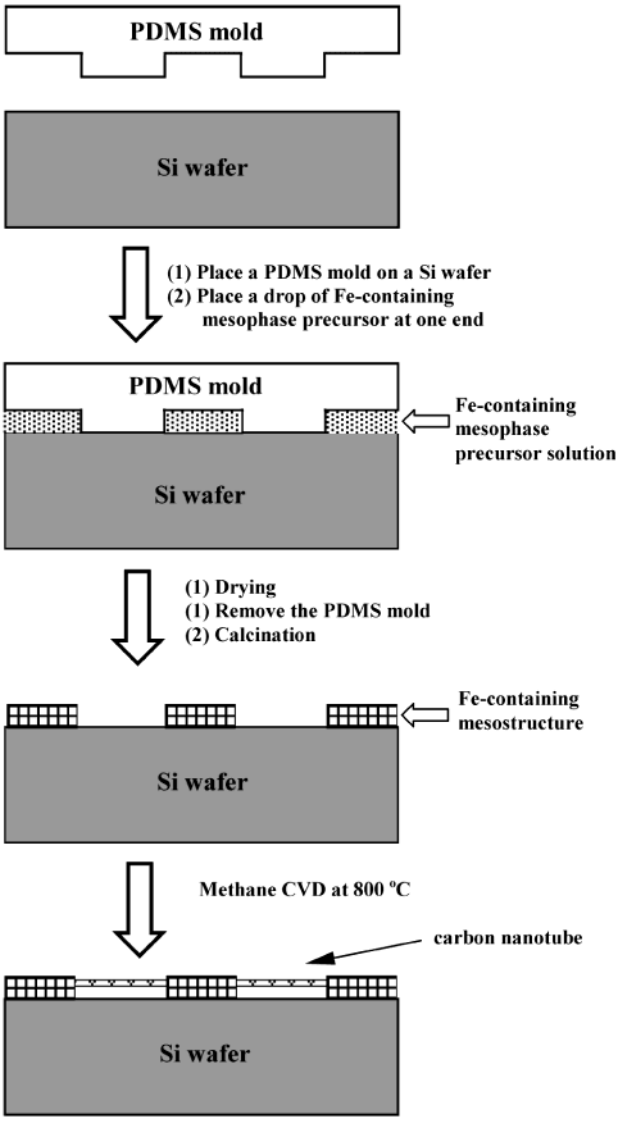

Figure 1. Schematic diagram of fabricating line-patterned mesostructure on a Si wafer for carbon nanotube growth.

XRD patterns (Figure 2a) show that at a low Fe doping level (Fe/Si = 0.8 mol %), the Fe/SBA-16 thin film preserves its mesostructure at up to 800 °C, though a large contraction of the cubic structure occurs. Only one strong diffraction peak (200) can be observed from the XRD pattern, indicating the formation of an orientationally ordered 3D structure (whose (100) plane is aligned parallel to the substrate).[18,19] The high thermal stability is further demonstrated by high-resolution SEM (HRSEM) images (Figure 2 inset and Figures 3a and 3b), which show well-ordered pore structure with mesopore dimension of around 5.4 nm (which is comparable to SWNT size). However, a higher doping level (Fe/Si = 5 mol % or higher) leads to a decrease in mesoporous ordering, and it results in deformation of the ordered mesopore structure with some bigger pores formed (Supporting Information s-Figure 1, XRD and SEM). High-angle XRD patterns of the corresponding powder samples (Figure 2b and Supporting Information s-Figure 1) indicate that no obvious diffraction peaks can be observed for Fe species over a wide loading range after 800 °C treatment (Fe/Si molar

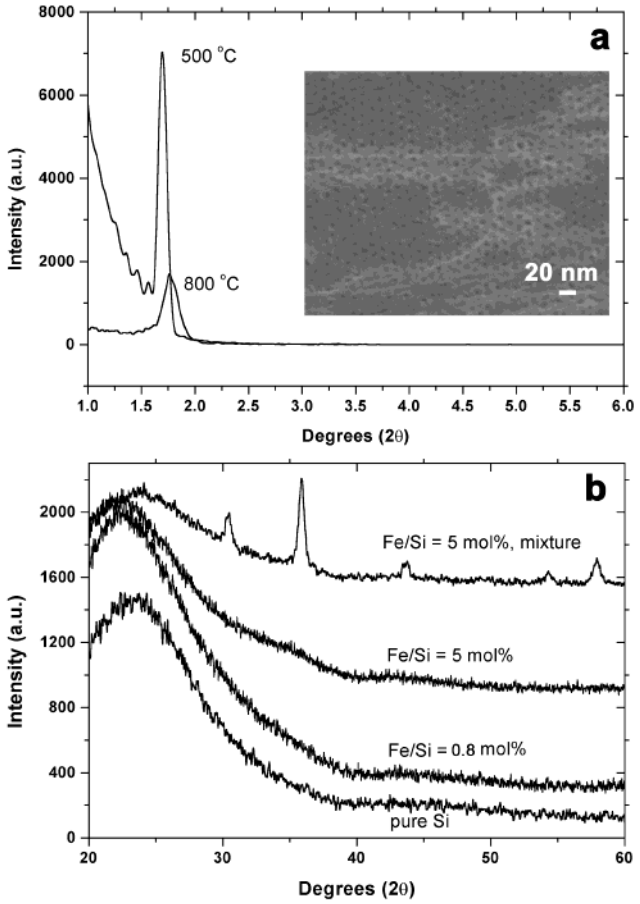

Figure 2. (a) XRD patterns of mesoporous Fe/SBA-16 (Fe/Si = 0.8 mol %) thin film at high temperatures, (inset) SEM image of Fe/SBA-16 thin film after 800 °C treatment. (b) XRD patterns of mesoporous Fe/SBA-16 powders with different molar ratios of Fe/Si. As a reference, the mixture here is referred as a mixture of SBA-16 powder and ~10 nm γ-Fe_2O_3.

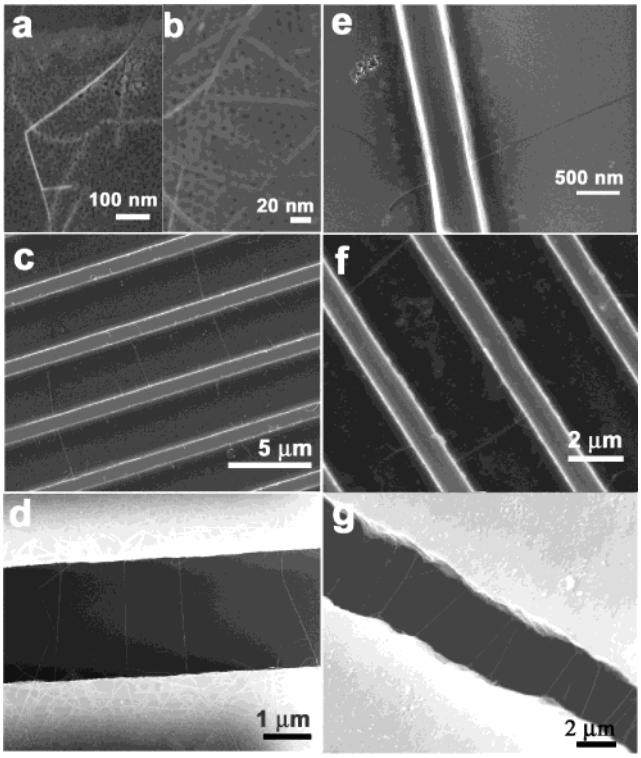

Figure 3. SEM images of carbon nanotubes (CNTs) grown from Fe-doped (Fe/Si = 0.8 mol %) mesoporous SiO_2 thin films. (a) Top surface of Fe/SBA-16 thin film which has a 3D pore mesostructure with CNTs emerging directly from the pores of the mesostructured template. (b) CNTs on the template surface. (c) CNTs grown from line micropatterns of an Fe/SBA-16 thin film on a silicon substrate, prepared according to the schematic shown in Figure 1. (d) Fe/SBA-16 thin film showing parallel CNTs growing across the microcrack, perpendicular to the direction of the trench. (e,f) CNTs grown from line micropatterns of an Fe/SBA-15 (1D pore mesostructure) thin film on a silicon substrate, prepared according to the schematic shown in Figure 1. (g) Fe/SBA-15 thin film showing CNTs spaced 1−2 μm apart growing across the microcrack. It is clear from the image that the CNTs are emerging from the sidewall of the template mesostructure. To visualize the carbon nanotubes, samples c, f, and g were coated with thin layers of gold. The images a, b, d, and e are from uncoated samples.

ratio of 0.8−30%), suggesting the high dispersion of nanometer-sized Fe species (α-Fe_2O_3 phase formed after calcination at higher than 550 °C) in the mesostructure with particle size probably smaller than the mesopore dimension. Because the mesoporous SiO_2 thin film has less external surface area compared with the high internal surface area, it can be reasonably proposed that almost all the Fe nanoparticles are distributed within mesoporous channels. Similar results were obtained for low Fe-doping SBA-15 with 1D in-plane pore channels and SBA-11 with 3D pore channels.

Scanning electron microscopy (SEM) images of carbon nanotubes grown from various mesoporous SiO_2 thin films (Figure 3) show a series of parallel trenches, constructed by soft lithography or formed by surface microcracks. The microcracks are of interest because the opposite lateral faces in the cracks used to be connected and become separate after crack formation with pore direction matching on each side of the crack. It is shown that the growth of carbon nanotubes usually starts from the 3D channels of Fe/SBA-16 (Figures 3a and 3b) or 1D in-plane channels of Fe/SBA-15 (Figure 3e) where catalysts are located and then beyond the channels. For Fe/SBA-16 with straight pore opening on each surface (Figures 3c and 3d), the nanotubes emerge either from the thin sidewall or from the top surface. Lateral growth allows the nanotubes to escape from strong van der Waals interactions from the surface with tube direction almost normal to the sidewall (parallel to the direction of the pore channels) (Figures 3c and 3d).[21] Some carbon nanotubes grow freely across the trenches until they touch adjacent walls (with spacings up to 3 μm), while some CNTs end up resting on the Si substrate surface (the oxide layer), which in both cases results in a parallel assembly of the nanotubes. The CNTs in contact with the surface are more clearly imaged by SEM at higher magnifications (Figure 3e). In direct contrast, CNTs which grow from the top surface of mesoporous Fe/SBA-16 tend to extend parallel to the surface partly due to the strong van der Waals interactions between surface and tubes (Figures 3a,b, and d). They probably grow vertically from the mesopores for some distance, and then may simply flop down or get entangled with nearby tubes. These nanotubes show no specific orientation compared with those from lateral

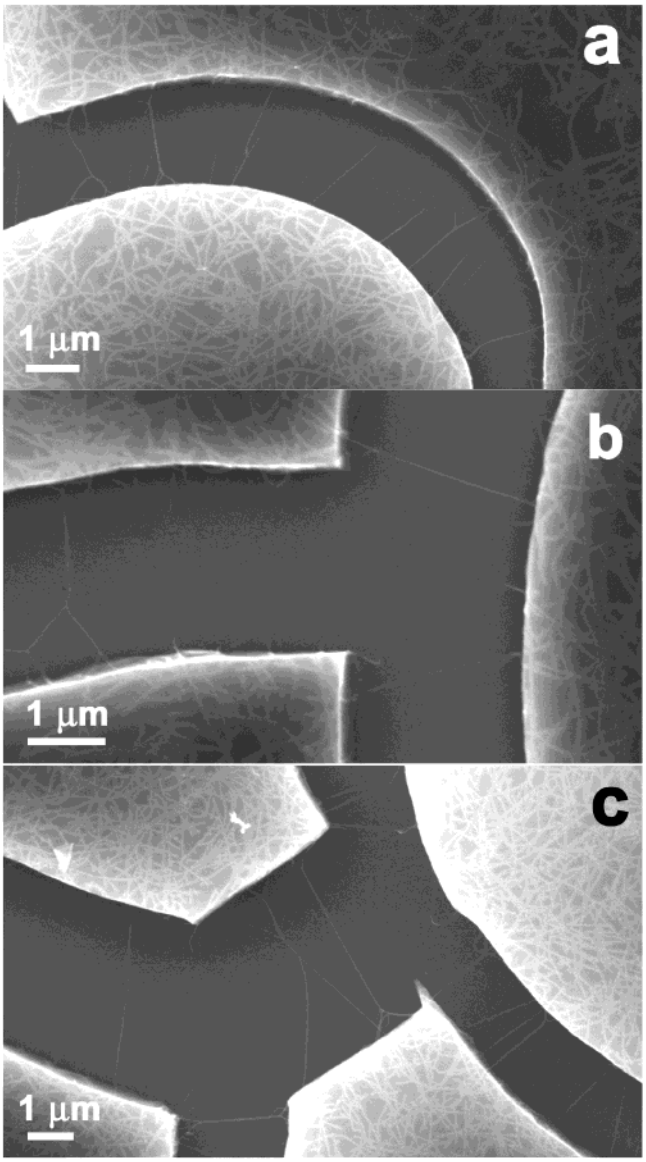

Figure 4. SEM images (with no gold coating) of typical carbon nanotube (CNT) assemblies grown from thin films of Fe/SBA-16 on a silicon substrate. CNTs can be observed growing across the surface and from the walls across the trenches. (a) A two-piece configuration. The series of carbon nanotubes clearly follows the radial curvature of the template mesostructure. (b) A three-piece configuration with a T-junction shaped trench with CNTs growing in a symmetrical pattern from each wall. (c) A four-piece configuration showing greater complexity in the array of carbon nanotube growth. Y-Junctions of coupled CNTs can be observed.

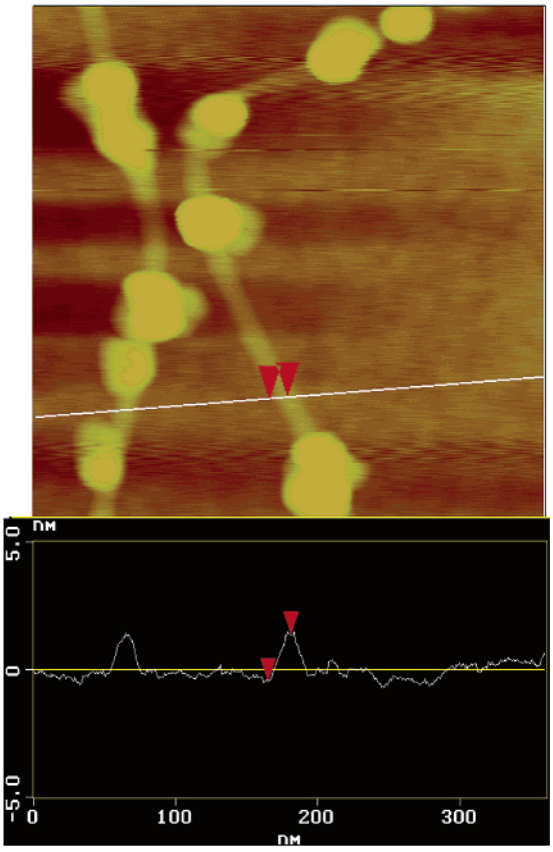

Figure 5. AFM topography image of nanotubes from mesoporous Fe/SBA-11 after HF treatment and corresponding topographic height measurements for the nanotubes.

growth. Some of these CNTs grow further across the adjacent trenches, which may randomize the parallel assembly (Figure 3d). Similar phenomena can also be found in Figure 4. In contrast to the 3D mesostructure of Fe/SBA-16, Fe/SBA-15 has in-plane mesoporous channels with 1D cylindrical mesopores. Nanotubes can only grow from the sidewall where there are only pore openings for Fe/SBA-15 thin film, and there are only a few tubes grown from the top surface (Figures 3e,f, and g). The lateral growth of carbon nanotubes also results in a parallel assembly over the parallel trenches (Figures 3f and 3g). In addition, the nanotube yield is a little lower for the Fe/SBA-15 thin film, possibly because the 1D cylindrical pores restrict diffusion of methane. Similarly, a parallel assembly of carbon nanotubes can be created on a line-patterned Fe/SBA-11 thin film, which has 3D pore channels. The above results indicate that since the growth of nanotubes starts from uniform and ordered mesoporous channels, pore direction in the thin film can control the orientation of the tubes at the early stage when they extrude from the pore channels and further result in an aligned assembly.

The lateral growth across the trenches could result in complex nanotube assemblies on curved two-piece (Figure 4a), three-piece (Figure 4b), and four-piece configurations (Figure 4c) with the tube orientations reflected by the pore directions of each piece of mesoporous SiO_2 thin film (Fe/SBA-16). These configurations are produced by microcracks on the thin film. It is worth mentioning that Figure 4a shows that CNTs follow the radial curvature of the trench, which is a strong indication of the orientation dependence upon the host matrix (Fe/SBA-16). It is also noted that carbon nanotubes grown from the top surface of the film do not show any orientation. Moreover, nanotube multiterminal junctions such as "Y", "L", and "H" can be generated (Figure 4, s-Figure 2), especially the Y junctions. These junctions are of great interest for their potential use in nanoscale CNT transistor or amplifier applications.[22,23] The above results indicate that by carefully designing micropatterns on a

mesoporous SiO_2 thin film, it may be possible to intentionally engineer more complex nanotube assemblies and nanotube junctions.

Atomic force microscopy (AFM) was used for accurate diameter determination by imaging directly onto the sample after HF solution was used to remove mesoporous SiO_2 matrix, while attempting to keep the nanotubes in place. This was performed by adding ~1 drop of HF aqueous solution (20 wt%) onto a known region on the substrate followed by removal of the residual solution after 5−10 min. In HF-washed samples of Fe/SBA-11, -15, and -16, diameters corresponding to published values for SWNTs were observed. Figure 5 shows a typical AFM image of nanotubes grown from cubic Fe/SBA-11, and the nanotube sizes were inferred from their topographic heights (large particles in the AFM images are likely undissolved SiO_2 matrix). The AFM results show that the nanotubes grown from Fe/SBA-16 thin film have diameters of ~2−4 nm, with the mean tube size of 2.5−3.5 nm. This was confirmed by a preliminary TEM survey of the etched material. The diameters of nanotubes observed tend to be smaller than the pore size of Fe/SBA-16 (~5.4 nm). CNTs with diameters larger than the pore size were not observed. For nanotubes grown from Fe/SBA-11 with smaller pore size (~3.5 nm), the AFM image in Figure 5 shows that the diameters of individual nanotubes are among 1−2.5 nm (with a mean pore size of 1.5−2 nm), smaller than those from Fe/SBA-16. Fe/SBA-11 may not be as stable as Fe/SBA-15 or Fe/SBA-16 at 800 °C, but the smaller pore size apparently yields smaller diameter nanotubes, suggesting that the pore size of mesoporous SiO_2 can control the dimension of carbon nanotubes.

In conclusion, we have reported a simple method for producing parallel assemblies of carbon nanotubes from parallel trenches using Fe-catalyzed methane CVD growth within thermally stable mesoporous SiO_2 (with a 3D or 1D porous architecture). The thin films of the mesoporous silica act as a template that allows lateral growth of CNTs that exert control over tube orientation and diameter (1−4 nm range) through the actual orientation of the pores and the pore diameter. The flexibility of constructing various nanotube assemblies and nanotube junctions suggests a potential of this procedure for controlled CNT growth for making future integrated electronic nanodevices, and demonstrates the ability to combine nanostructured thin films, prepared by chemical methods, with conventional patterning techniques. A procedure for making complex oriented assemblies of CNTs on a predesigned micropatterned mesoporous SiO_2 thin film is currently under way.

Acknowledgment. This work was supported primarily by the MRSEC program of the National Science Foundation under award number DMR-0213574, and in part by the Nanoscale Science and Engineering Initiative of the National Science Foundation under NSF award number CHE-0117752. The authors thank Prof. Louis Brus and Dr. Ken Bosnick for useful discussions and assistance with facilities.

Supporting Information Available: XRD patterns and HRSEM images of Fe/SBA-16 powders (s-Figure1) and SEM images of nanotube junctions (s-Figure 2). This material is available free of charge via the Internet at http://pubs.acs.org.

Note Added after ASAP Posting. This article was released ASAP on 2/5/2003. The article was reposted on 2/7/2003 with a new Table of Contents graphic.

References

(1) Dai, H. J. *Surf. Sci.* **2002**, *500*, 218.
(2) Avouris, Ph. *Acc. Chem. Res.* **2002**, *35*, 1026.
(3) Ouyang, M.; Huang, J. L.; Lieber, C. M. *Acc. Chem. Res.* **2002**, *35*, 1018.
(4) Wind, S. J.; Appenzeller, J.; Martel, R.; Derycke, V.; Avouris, Ph. *Appl. Phys. Lett.* **2002**, *80*, 3817.
(5) Zheng, F.; Liang, L.; Gao, Y. F.; Sukamto, J. H.; Aardahl, C. L. *Nano Lett.* **2002**, *2*, 729.
(6) Zheng, G. F.; Zhu, H. G.; Luo, Q.; Zhou, Y. M.; Zhao, D. Y. *Chem. Mater.* **2001**, *13*, 2240.
(7) Li, W. Z.; Xie, S. S.; Qian, L. X.; Chang, B. H.; Zou, B. S.; Zhou, W. Y.; Zhao, R. A.; Wang, G. *Science* **1996**, *274*, 1701.
(8) Li, J.; Papadopoulos, C.; Xu, J. M.; Moskovits, M. *Appl. Phys. Lett.* **1999**, *75*, 367.
(9) Cassell, A. M.; Verma, S.; Delzeit, L.; Meyyappan, M.; Han, J. *Langmuir* **2001**, *17*, 260.
(10) Zhu, H. W.; Xu, C. L.; Wu, D. H.; Wei, B. Q.; Vajtai, R.; Ajayan, P. M. *Science* **2002**, *296*, 884.
(11) Cassell, A. M.; Franklin, N. R.; Tombler, T. W.; Chan, E. M.; Han, J.; Dai, H. J. *J. Am. Chem. Soc.* **1999**, *121*, 7975.
(12) Joselevich, E.; Lieber, C. M. *Nano Lett.* **2002**, *2*, 1137.
(13) Zhang, Y. G.; Chang, A. L.; Cao, J.; Wang, Q.; Kim, W.; Li, Y. M.; Morris, N.; Yenilmez, E.; Kong, J.; Dai, H. J. *Appl. Phys. Lett.* **2001**, *79*, 3155.
(14) Harutyunyan, A. R.; Pradhan, B. K.; Kim, U. J.; Chen, G. G.; Eklund, P. C. *Nano Lett.* **2002**, *2*, 525.
(15) Li, Y. M.; Kim, W.; Zhang, Y. G.; Rolandi, M.; Wang, D. W.; Dai, H. J. *J. Phys. Chem. B* **2001**, *105*, 11424.
(16) Cheung, C. L.; Kurtz, A.; Park, H.; Lieber, C. M. *J. Phys. Chem. B* **2002**, *106*, 2429.
(17) Li, Y.; Liu, J.; Wang, Y. Q.; Wang, Z. L. *Chem. Mater.* **2001**, *13*, 1008.
(18) Alberius, P. C. A.; Frindell, K. L.; Hayward, R. C.; Kramer, E. J.; Stucky, G. D.; Chmelka, B. F. *Chem. Mater.* **2002**, *14*, 3284.
(19) Zhao, D. Y.; Yang, P. D.; Melosh, N.; Feng, J. L.; Chmelka, B. F.; Stucky, G. D. *Adv. Mater.* **1998**, *10*, 1380.
(20) Yang, P. D.; Deng, T.; Zhao, D. Y.; Feng, P. Y.; Pine, D.; Chmelka, B. F.; Whitesides, G. M.; Stucky, G. D. *Science* **1998**, *282*, 2244.
(21) Wind, S. J.; Martel, R.; Avouris, Ph. *J. Vac Sci. Technol. B* **2002**, *20*, 2745.
(22) Andriotis, A. N.; Menon, M.; Srivastava, D.; Chernozatonskii, L. *Phys. Rev. B* **2002**, *65*, 165416.
(23) Li, J.; Papadopoulos, C.; Xu, J. *Nature* **1999**, *402*, 253.

NL025880P